

# Simultaneously accounting for winner's curse and sample structure in Mendelian randomization: bivariate rerandomized inverse variance weighted estimator

Xin Liu,<sup>a</sup> Ping Yin,<sup>a\*</sup> and Peng Wang<sup>a\*</sup>

<sup>a</sup>Department of Epidemiology and Biostatistics, School of Public Health,  
Tongji Medical College, Huazhong University of Science and Technology,  
Wuhan, China

March 9, 2026

---

\*Contact pingyintj2000@126.com or pengwang\_stat@hust.edu.cn

## Abstract

The recently developed rerandomized inverse variance weighted (RIVW) estimator provides a simple and efficient framework to break the winner’s curse in two-sample Mendelian randomization (MR). However, this method has ignored the possible presence of sample structure (e.g., residual population stratification and sample overlap), a common confounding factor in MR studies. Sample structure can not only distort SNP–exposure and SNP–outcome association estimates but also induce correlation between them, leading exposure-side instrument selection to propagate bias to the outcome side. To address this challenge, we propose the bivariate RIVW (BRIVW) estimator that can simultaneously account for the winner’s curse and sample structure. The BRIVW estimator extends the RIVW framework by modeling the joint distribution of SNP–exposure and SNP–outcome associations, first adjusting their covariance matrix via linkage disequilibrium score regression to account for sample structure, and then applying randomized instrument selection and Rao–Blackwellization to obtain unbiased post-selection association estimates as well as their covariance matrix. Under appropriate conditions, we show that the BRIVW estimator is consistent and asymptotically normal. Extensive simulations and real data analyses demonstrate that the BRIVW estimator provides more accurate causal effect estimates than existing methods.

*Keywords:* causal inference, inverse variance weighting, sample structure, two-sample Mendelian randomization, winner’s curse

# 1 Introduction

Establishing causal relationships remains a central goal in biomedical research (Rothman and Greenland 2005). Randomized controlled trials (RCTs) are considered the gold standard for establishing causal relationships (Jones and Podolsky 2015), but their execution is frequently limited by significant costs, ethical dilemmas, or practical challenges (Bonde-mark and Ruf 2015). Mendelian randomization (MR) provides an attractive alternative by leveraging genetic variants—typically single nucleotide polymorphisms (SNPs)—as instrumental variables (IVs) to infer causal effects using observational data (Smith and Ebrahim 2003; Didelez and Sheehan 2007; Burgess et al. 2012). The rapid expansion of genome-wide association studies (GWAS) has substantially enhanced the feasibility and power of two-sample MR but has also exposed several important sources of bias beyond pleiotropy.

Among these, weak IVs and the winner’s curse have attracted increasing attention. Weak IV bias occurs when the SNP-exposure associations are weak enough to make the measurement error non-negligible, resulting in a shift of the causal estimate toward the null (Zhao et al. 2020; Ye, Shao, and Kang 2021). The debiased inverse variance weighted (dIVW) estimator (Ye, Shao, and Kang 2021) and their extensions (Xu et al. 2023; Su et al. 2024) formally tackled weak IV bias. To improve statistical power, practitioners often select IVs based on their association strength with the exposure. However, using the same data for selection and estimation can bias SNP-exposure effects, a phenomenon known as the winner’s curse, also causing downward bias in causal estimates (Gkatzionis and Burgess 2019; Jiang et al. 2023). The recently proposed rerandomized IVW (RIVW) estimator (Ma, Wang, and Wu 2023) addresses this issue by combining randomized IV selection with Rao–Blackwellization, providing a simple and effective correction for both weak IV bias and the winner’s curse in two-sample MR.

Nevertheless, RIVW and related methods implicitly assume the absence of sample structure. In practice, sample structure—including population stratification, cryptic relatedness, and sample overlap—is ubiquitous in GWAS data even after adjustment using principal component (Price et al. 2006) analysis and linear mixed models (Loh et al. 2015). Sample structure not only distorts SNP–exposure and SNP–outcome association estimates but also induces correlation between them (Hu et al. 2022). This correlation allows exposure-side

IV selection to propagate bias to the outcome side, resulting in a two-sided winner’s curse problem. In the presence of weak IVs, this distortion is further amplified and can lead to spurious causal findings. Recent studies have highlighted the severity of outcome-side winner’s curse under such conditions (Sadreev et al. 2021; Jiang et al. 2023), yet practical methods that jointly address winner’s curse and sample structure remain limited. Although MR-APSS (Hu et al. 2022) simultaneously accounts for sample structure and the winner’s curse, it relies on strong modeling assumptions, violations of which can lead to inflated false positives or reduced statistical power (Xie et al. 2025). Furthermore, MR-APSS lacks a closed-form solution and requires computationally intensive variational inference, limiting its applicability in large-scale MR analyses.

To address this gap, we propose the bivariate RIVW (BRIVW) estimator that extends the RIVW framework to explicitly model the joint distribution of SNP–exposure and SNP–outcome associations. We first adjust the covariance matrix of these associations using linkage disequilibrium score regression (LDSC) to account for sample structure (Bulik-Sullivan et al. 2015a, b; Hu et al. 2022), and then apply randomized IV selection and Rao–Blackwellization to obtain unbiased post-selection association estimates as well as their covariance matrix. This bivariate extension allows us to simultaneously account for weak IV bias, two-sided winner’s curse, and sample structure within a simple and efficient IVW framework.

On the theoretical side, we prove that our proposed BRIVW estimator is consistent and asymptotically normal under some regular conditions. The BRIVW estimator can utilize a more liberal threshold to improve power, as it eliminates both weak IV bias and the two-sided winner’s curse. Moreover, we derive a consistent standard error based on the regression interpretation of BRIVW, which retains the same analytical form irrespective of balanced horizontal pleiotropy, reducing the practical burden of assumption selection. Furthermore, after accounting for spurious trait associations induced by sample structure, the Instrument Strength Independent on Direct Effect (InSIDE) assumption underlying balanced pleiotropy becomes more plausible at the estimation level. On the practical side, building on the simple and efficient IVW framework while effectively accounting for the three major sources of bias, BRIVW demonstrates well-controlled type I error, high

statistical power, and accurate causal effect estimates in both simulations and real data applications.

The remainder of the article is organized as follows. Section 2 introduces the notation and assumptions. Section 3 reviews the IVW family of methods and examines the impact of sample structure on their performance. Section 4 characterizes the joint bias arising from weak IVs, the winner’s curse, and sample structure, and presents the proposed BRIVW estimator together with its theoretical properties. Sections 5 and 6 report simulation results and real data applications, respectively. Section 7 concludes with a discussion.

## 2 Notations and Assumptions

We consider the standard two-sample MR framework based on GWAS summary statistics. After LD pruning or clumping (Purcell et al. 2007; Hemani et al. 2018), suppose that  $p$  independent SNPs  $G_1, \dots, G_p$  are available as candidate IVs. Let  $\beta$  denote the causal effect of an exposure  $X$  on an outcome  $Y$ . A commonly adopted linear structural model (Pierce and Burgess 2013; Bowden et al. 2017; Burgess, Small, and Thompson 2017) is given by

$$X = \sum_{j=1}^p \gamma_j G_j + \beta_{UX} U + E_X, \quad (1)$$

$$Y = \beta X + \beta_{UY} U + E_Y, \quad (2)$$

where  $\gamma_j$  denotes the effect of SNP  $G_j$  on  $X$ , and  $U$  is an unmeasured confounder independent of all  $G_j$ .  $E_X$  and  $E_Y$  are mutually independent error terms that are also independent of  $(G_1, \dots, G_p, U)$ . Let  $\Gamma_j$  denote the marginal effect of  $G_j$  on  $Y$ ; under the model above,  $\Gamma_j = \beta \gamma_j$ . To allow for the valid inference of  $\beta$ , the SNPs  $G_1, \dots, G_p$  are required to satisfy the following IV assumptions (Sanderson et al. 2022): (i) relevance:  $\gamma_j \neq 0$  for at least some  $j$ ; (ii) independence:  $G_j \perp U$  for all  $j$ ; and (iii) exclusion restriction:  $G_j$  affects  $Y$  only through  $X$ .

Because individual-level data are often unavailable, two-sample MR is typically conducted using GWAS summary statistics (Burgess et al. 2015). Specifically, for each SNP  $G_j$ , we observe marginal association estimates  $(\hat{\gamma}_j, \tilde{\sigma}_{\hat{\gamma}_j})$  from the exposure GWAS and  $(\hat{\Gamma}_j, \tilde{\sigma}_{\hat{\Gamma}_j})$  from the outcome GWAS, where  $\tilde{\sigma}_{\hat{\gamma}_j}$  and  $\tilde{\sigma}_{\hat{\Gamma}_j}$  denote the standard errors from

the original GWAS summary statistics, prior to any adjustment for sample structure using LDSC.

In the ideal two-sample MR setting, the exposure and outcome GWAS are conducted in independent samples drawn from homogeneous populations, so that  $\hat{\gamma}_j$  and  $\hat{\Gamma}_j$  are independent (Zhao et al. 2020; Ye, Shao, and Kang 2021; Ma, Wang, and Wu 2023). In modern applications based on large biobank data, however, population stratification, cryptic relatedness, and sample overlap are ubiquitous. These forms of sample structure may inflate the variance of  $\hat{\gamma}_j$  and  $\hat{\Gamma}_j$  and induce correlation between them (Burgess, Davies, and Thompson 2016; Hu et al. 2022; Zhang et al. 2025). To accommodate such settings, we adopt the following assumptions:

**Assumption 1.** *The exposure and outcome GWAS sample sizes, denoted by  $n_X$  and  $n_Y$ , satisfy  $n_X, n_Y \rightarrow \infty$  at the same order, and the number of independent SNPs  $p \rightarrow \infty$ .*

**Assumption 2.** *(i) For any  $j \neq j'$ , the pairs  $(\hat{\gamma}_j, \hat{\Gamma}_j)$  and  $(\hat{\gamma}_{j'}, \hat{\Gamma}_{j'})$  are mutually independent.*

*(ii) For each SNP  $j$ ,*

$$\begin{bmatrix} \hat{\gamma}_j \\ \hat{\Gamma}_j \end{bmatrix} \sim N \left( \begin{bmatrix} \gamma_j \\ \Gamma_j \end{bmatrix}, \begin{bmatrix} \sigma_{\hat{\gamma}_j}^2 & \rho \sigma_{\hat{\gamma}_j} \sigma_{\hat{\Gamma}_j} \\ \rho \sigma_{\hat{\gamma}_j} \sigma_{\hat{\Gamma}_j} & \sigma_{\hat{\Gamma}_j}^2 \end{bmatrix} \right).$$

*where  $\rho$  captures the correlation induced by sample structure. In addition, there exists some  $v \rightarrow 0$ , such that  $\{\sigma_{\hat{\gamma}_j}/v, \sigma_{\hat{\Gamma}_j}/v : 1 \leq j \leq p\}$  are bounded and bounded away from zero.*

**Remark.** In the presence of sample structure, the reported standard errors  $\tilde{\sigma}_{\hat{\gamma}_j}$  and  $\tilde{\sigma}_{\hat{\Gamma}_j}$  may underestimate the true sampling variability. Following Hu et al. (2022), we introduce variance inflation factors  $c_1$  and  $c_2$  and define  $\sigma_{\hat{\gamma}_j} = c_1 \tilde{\sigma}_{\hat{\gamma}_j}$  and  $\sigma_{\hat{\Gamma}_j} = c_2 \tilde{\sigma}_{\hat{\Gamma}_j}$ . The correlation parameter is written as  $\rho = c_{12}/\sqrt{c_1 c_2}$ , where  $c_{12}$  captures cross-trait correlation induced by sample structure. The quantities  $c_1$ ,  $c_2$ , and  $c_{12}$  can be consistently estimated from the intercepts of single-trait and bivariate LDSC and are treated as known constants in the subsequent analysis (Liu and Lin 2018; Hu et al. 2022).

To facilitate the subsequent discussion, we define the average strength of the IVs as

$$\kappa = \frac{1}{p} \sum_{j=1}^p \left( \frac{\gamma_j}{\sigma_{\hat{\gamma}_j}} \right)^2.$$

We also introduce the following notation for probabilistic ordering. We use  $\xrightarrow{p}$  and  $\xrightarrow{d}$  to denote convergence in probability and convergence in distribution, respectively. For random variables  $A$  and  $B$ , the notation  $A = O_p(B)$  indicates that  $A/B$  is bounded in probability, whereas  $A = o_p(B)$  signifies that  $A/B \xrightarrow{p} 0$ .

### 3 Overview of IVW family of methods

#### 3.1 Prior work in IVW family of methods

In this section, we first review the IVW (Didelez and Sheehan 2007) estimator and its two notable extensions, dIVW (Ye, Shao, and Kang 2021) and RIVW (Ma, Wang, and Wu 2023), which form the foundation of our methodological development. The IVW method estimates  $\beta$  by a weighted regression of  $\hat{\Gamma}_j$  on  $\hat{\gamma}_j$ :

$$\hat{\beta}_{\text{IVW}} = \frac{\sum_{j=1}^p \hat{\Gamma}_j \hat{\gamma}_j / \sigma_{\hat{\Gamma}_j}^2}{\sum_{j=1}^p \hat{\gamma}_j^2 / \sigma_{\hat{\Gamma}_j}^2}.$$

Since the IVW estimator is biased toward zero due to the estimation error in  $\hat{\gamma}_j$ , the dIVW estimator corrects this by replacing the denominator with  $\sum_{j=1}^p (\hat{\gamma}_j^2 - \sigma_{\hat{\gamma}_j}^2) / \sigma_{\hat{\Gamma}_j}^2$ . The resulting estimator,

$$\hat{\beta}_{\text{dIVW}} = \frac{\sum_{j=1}^p \hat{\Gamma}_j \hat{\gamma}_j / \sigma_{\hat{\Gamma}_j}^2}{\sum_{j=1}^p (\hat{\gamma}_j^2 - \sigma_{\hat{\gamma}_j}^2) / \sigma_{\hat{\Gamma}_j}^2},$$

is more robust under many weak IVs. However, to improve inference efficiency, practitioners typically select a set of IVs that satisfy  $|\hat{\gamma}_j / \sigma_{\hat{\gamma}_j}| > \lambda$ , where  $\lambda$  is a pre-specified cutoff value. This practice introduces the winner’s curse into MR analyses, by distorting the distribution of  $\hat{\gamma}_j$  into a truncated normal, which systematically overestimates the true effect  $\gamma_j$ . To mitigate this issue, Ma et al. (2023) introduce a pseudo SNP–exposure effect  $Z_j \sim N(0, \eta^2)$  and perform randomized selection:

$$S_\lambda = \{j : S_j > 0, j = 1, 2, \dots, p\}, \quad \text{where } S_j = \left| \frac{\hat{\gamma}_j}{\sigma_{\hat{\gamma}_j}} + Z_j \right| - \lambda.$$

Here,  $\eta$  is a pre-specified constant reflecting the noise level of the pseudo SNPs. The key idea of RIVW is to construct an unbiased SNP–exposure effect that is independent of the selection indicator  $S_j$ . Using the Rao–Blackwell theorem to improve efficiency, yields the following bias-corrected SNP–exposure effect:

$$\hat{\gamma}_{j,\text{RB}} = \hat{\gamma}_j - \frac{\sigma_{\hat{\gamma}_j}}{\eta} \frac{\phi(A_{j,+}) - \phi(A_{j,-})}{1 - \Phi(A_{j,+}) + \Phi(A_{j,-})}, \quad \text{where } A_{j,\pm} = -\frac{\hat{\gamma}_j}{\sigma_{\hat{\gamma}_j}\eta} \pm \frac{\lambda}{\eta},$$

and  $\phi(\cdot)$  and  $\Phi(\cdot)$  denote the probability density function and cumulative distribution function of the standard normal distribution, respectively. The  $\hat{\gamma}_{j,\text{RB}}$  is unbiased and achieves minimum variance for a given  $\eta$ . Incorporating  $\hat{\gamma}_{j,\text{RB}}$  and its variance  $\hat{\sigma}_{\hat{\gamma}_{j,\text{RB}}}^2$  into the dIVW estimator yields the RIVW estimator:

$$\hat{\beta}_{\text{RIVW}} = \frac{\sum_{j \in S_\lambda} \hat{\Gamma}_j \hat{\gamma}_{j,\text{RB}} / \sigma_{\hat{\Gamma}_j}^2}{\sum_{j \in S_\lambda} (\hat{\gamma}_{j,\text{RB}}^2 - \hat{\sigma}_{\hat{\gamma}_{j,\text{RB}}}^2) / \sigma_{\hat{\Gamma}_j}^2},$$

which corrects both selection bias and weak IV bias. Notably, the IVW, dIVW, and RIVW estimators are all derived under the ideal two-sample MR setting without sample structure, corresponding to  $c_1 = 1$ ,  $c_2 = 1$ , and  $\rho = 0$  in Assumption 2. When this assumption is violated, as often occurs in practice, their theoretical properties no longer hold, and they may yield biased causal estimates.

### 3.2 Impact of sample structure on IVW family of methods

To isolate the impact of correlation induced by sample structure, we consider a simplified setting under Assumption 2 with  $c_1 = c_2 = 1$  and  $\rho \neq 0$ . With some algebraic manipulation (See Appendix S2), the IVW estimator can be expressed as

$$\hat{\beta}_{\text{IVW}} = \beta + \frac{\sum_{j=1}^p (\rho \sigma_{\hat{\gamma}_j} \sigma_{\hat{\Gamma}_j} - \beta \sigma_{\hat{\gamma}_j}^2) / \sigma_{\hat{\Gamma}_j}^2}{\sum_{j=1}^p (\gamma_j^2 + \sigma_{\hat{\gamma}_j}^2) / \sigma_{\hat{\Gamma}_j}^2} + o_p(1),$$

which reveals two distinct sources of bias: attenuation due to estimation error in  $\hat{\gamma}_j$  and an additional bias arising from the covariance between  $\hat{\gamma}_j$  and  $\hat{\Gamma}_j$  induced by sample structure. In particular, when  $\beta$  and  $\rho$  share the same sign, these biases may partially offset each other; otherwise, they compound. Similarly, the dIVW estimator removes weak IV bias but remains biased under sample structure (See Appendix S3):

$$\hat{\beta}_{\text{dIVW}} = \beta + \frac{\sum_{j=1}^p (\rho \sigma_{\hat{\gamma}_j} \sigma_{\hat{\Gamma}_j} / \sigma_{\hat{\Gamma}_j}^2)}{\sum_{j=1}^p (\gamma_j^2 / \sigma_{\hat{\Gamma}_j}^2)} + o_p(1).$$

Moreover, under the sample structure, the asymptotic normality of both IVW and dIVW estimators requires  $\kappa/p \rightarrow \infty$ , a stringent condition rarely satisfied in practice (See Appendix S2 and S3). More critically, sample structure also breaks the independence between  $\hat{\Gamma}_j$  and the randomized selection indicator  $S_j$ :

$$\text{Cov}\left(\hat{\Gamma}_j, \frac{\hat{\gamma}_j}{\sigma_{\hat{\gamma}_j}} + Z_j\right) = \rho\sigma_{\hat{\Gamma}_j} \neq 0 \implies \mathbb{E}[\hat{\Gamma}_j | S_j > 0] \neq \mathbb{E}[\hat{\Gamma}_j] = \Gamma_j.$$

Thus, sample structure propagates the winner's curse to the outcome side, inducing additional bias in the RIVW estimator. Motivated by this interaction between sample structure and selection bias, Section 4 formally characterizes their joint effect and introduces the BRIVW estimator to correct these biases simultaneously.

## 4 Method

### 4.1 Joint bias structure under sample structure and IV selection

Recall that  $\hat{\Gamma}_j$  is not independent of the selection indicator  $S_j$  under sample structure, so we derive the conditional distribution of  $\hat{\Gamma}_j$  given  $S_j > 0$  in the following lemma.

**Lemma 1.** *Assume that Assumption 2 holds. Then the conditional density of  $\hat{\Gamma}_j/\sigma_{\hat{\Gamma}_j}$  given the selection event  $S_j > 0$  is given by*

$$f_{\hat{\Gamma}_j/\sigma_{\hat{\Gamma}_j} | S_j > 0}(x) = \frac{1}{\Pr(S_j > 0)} \phi\left(x - \frac{\Gamma_j}{\sigma_{\hat{\Gamma}_j}}\right) \left[ \Phi\left(\frac{-\lambda - \frac{\gamma_j}{\sigma_{\hat{\gamma}_j}} + \frac{\rho\Gamma_j}{\sigma_{\hat{\Gamma}_j}} - \rho x}{\sqrt{1 - \rho^2 + \eta^2}}\right) + 1 - \Phi\left(\frac{\lambda - \frac{\gamma_j}{\sigma_{\hat{\gamma}_j}} + \frac{\rho\Gamma_j}{\sigma_{\hat{\Gamma}_j}} - \rho x}{\sqrt{1 - \rho^2 + \eta^2}}\right) \right].$$

where

$$\Pr(S_j > 0) = \Phi\left(\frac{-\lambda - \frac{\gamma_j}{\sigma_{\hat{\gamma}_j}}}{\sqrt{1 + \eta^2}}\right) + 1 - \Phi\left(\frac{\lambda - \frac{\gamma_j}{\sigma_{\hat{\gamma}_j}}}{\sqrt{1 + \eta^2}}\right).$$

Thus, the conditional expectation of  $\hat{\Gamma}_j$  given  $S_j > 0$  is

$$\mathbb{E}[\hat{\Gamma}_j | S_j > 0] = \Gamma_j + \underbrace{\frac{\rho\sigma_{\hat{\Gamma}_j}}{\Pr(S_j > 0)\sqrt{1 + \eta^2}} \left[ \phi\left(\frac{\lambda - \frac{\gamma_j}{\sigma_{\hat{\gamma}_j}}}{\sqrt{1 + \eta^2}}\right) - \phi\left(\frac{-\lambda - \frac{\gamma_j}{\sigma_{\hat{\gamma}_j}}}{\sqrt{1 + \eta^2}}\right) \right]}_{\text{bias}}$$

Lemma 1 shows that under sample structure ( $\rho \neq 0$ ), IV selection induces bias in  $\hat{\Gamma}_j$  through its correlation with  $\hat{\gamma}_j$ . The bias term reflects a joint effect of weak IVs, the winner’s curse, and sample structure; its magnitude and direction depend on  $\rho$  and are amplified for weaker IVs (i.e., smaller  $\gamma_j/\sigma_{\hat{\gamma}_j}$ ). Moreover, the covariance between  $\hat{\gamma}_j$  and  $\hat{\Gamma}_j$  after IV selection is challenging to quantify, complicating the sample structure bias correction in MR analyses.

Outcome-side winner’s curse is often more severe than exposure-side, as it more readily induces false positives (Sadreev et al. 2021; Jiang et al. 2023), yet it is largely overlooked in practice. In principle, the winner’s curse on both the exposure and outcome sides could be eliminated using three independent samples: one for IV selection, one for SNP–exposure estimation, and one for SNP–outcome estimation. However, such designs are rarely feasible in practice, as modern GWAS typically rely on large-scale meta-analyses that reuse overlapping cohorts and retain residual population structure.

To illustrate the complex interplay among weak IVs, the winner’s curse, and sample structure, we conduct two simulation studies. The first examines how this interplay distorts the distribution of  $\hat{\Gamma}_j$ , while the second evaluates its impact on bias in the IVW family of estimators.

**Example 1** We generate  $\hat{\gamma}_j/\sigma_{\hat{\gamma}_j}$  and  $\hat{\Gamma}_j/\sigma_{\hat{\Gamma}_j}$  from a bivariate normal distribution with means  $(\gamma_j/\sigma_{\hat{\gamma}_j}, \Gamma_j/\sigma_{\hat{\Gamma}_j})$ , unit marginal variances, and correlation coefficient  $\rho$ . The true normalized instrument effect  $\gamma_j/\sigma_{\hat{\gamma}_j}$  is varied over  $\{0.1\lambda, 0.5\lambda, 2\lambda\}$ , representing weak, moderate, and strong IVs, respectively, where  $\lambda = \Phi^{-1}(1 - 5 \times 10^{-5}/2)$ . We also set  $\Gamma_j/\sigma_{\hat{\Gamma}_j} = \gamma_j/\sigma_{\hat{\gamma}_j}$  and consider  $\rho \in \{-0.3, -0.1, 0, 0.1, 0.3\}$  to represent different levels of sample structure. From the generated data, we select SNPs based on the criterion  $S_j > 0$  with  $\eta = 0.5$  and  $\lambda$  as above, and then plot the empirical density of  $\hat{\Gamma}_j$  after selection. As shown in Figure 1, when there is no sample structure ( $\rho = 0$ ), the distribution of  $\hat{\Gamma}_j$  remains correctly centered regardless of IV strength. In contrast, when sample structure is present ( $\rho \neq 0$ ), the distribution of  $\hat{\Gamma}_j$  becomes distorted after IV selection, with the degree of distortion being more pronounced for both larger  $|\rho|$  values and weaker IVs. The direction of the distortion is determined by the sign of  $\rho$ . These results corroborate Lemma 1 and demonstrate how weak IVs, the winner’s curse, and sample structure jointly distort SNP–outcome associations

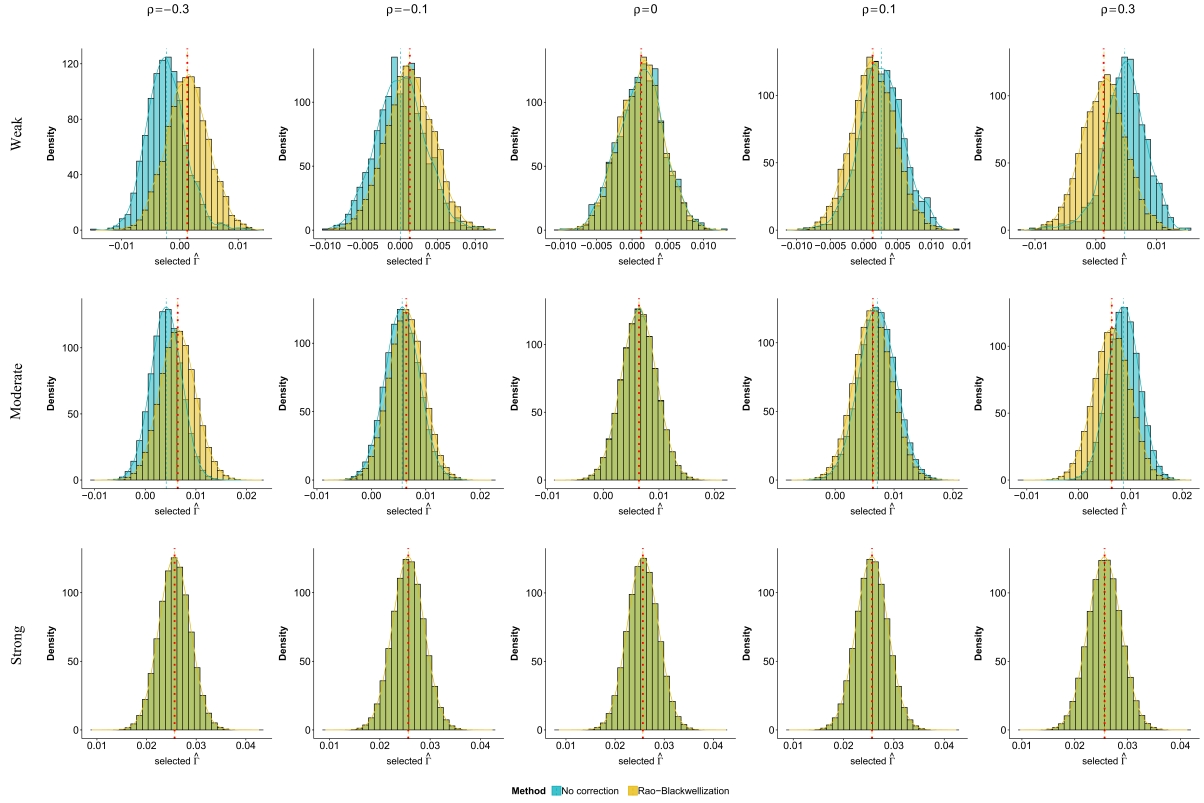


Figure 1: Comparison between  $\hat{\Gamma}_{j, \text{RB}}$  and  $\hat{\Gamma}_j$  after IV selection under different levels of sample structure ( $\rho$ ) and IV strength ( $\gamma_j/\sigma_{\hat{\gamma}_j}$ ). Weak, moderate, and strong instruments correspond to  $\gamma_j/\sigma_{\hat{\gamma}_j} \in \{0.1\lambda, 0.5\lambda, 2\lambda\}$ , where  $\lambda = \Phi^{-1}(1 - 5 \times 10^{-5}/2)$ . The red dotted lines indicate the true value of  $\Gamma_j$ .

after IV selection.

**Example 2** We generate 1000 Monte Carlo samples with the true causal effect  $\beta = 0.2$  and  $p = 200,000$  independent SNPs. The true SNP–exposure effects  $\gamma_j$  follow the mixture distribution:

$$\begin{pmatrix} \gamma_j \\ \alpha_j \end{pmatrix} \sim \underbrace{\pi_x(1 - \omega) \begin{pmatrix} N(0, \epsilon_x^2) \\ \delta_0 \end{pmatrix}}_{\text{Valid IVs}} + \underbrace{\pi_x\omega \begin{pmatrix} N(0, \epsilon_x^2) \\ N(0, \tau^2) \end{pmatrix}}_{\text{Balanced pleiotropy}} + \underbrace{\pi_y \begin{pmatrix} \delta_0 \\ N(0, \tau^2) \end{pmatrix}}_{\text{Outcome-only effects}} + \underbrace{(1 - \pi_x - \pi_y) \begin{pmatrix} \delta_0 \\ \delta_0 \end{pmatrix}}_{\text{Purely null SNPs}}, \quad (3)$$

and the true SNP–outcome effects are given by  $\Gamma_j = \beta\gamma_j + \alpha_j$ . Here,  $\pi_x$  and  $\pi_y$  denote the proportions of SNPs associated with the exposure and outcome, respectively;  $\omega$  controls the proportion of SNPs exhibiting balanced pleiotropy;  $\epsilon_x^2$  and  $\tau^2$  are the variances of SNP

effects on the exposure and outcome, respectively; and  $\delta_0$  is the Dirac measure centred at zero. Similar data generation models have been widely used in the MR literature.

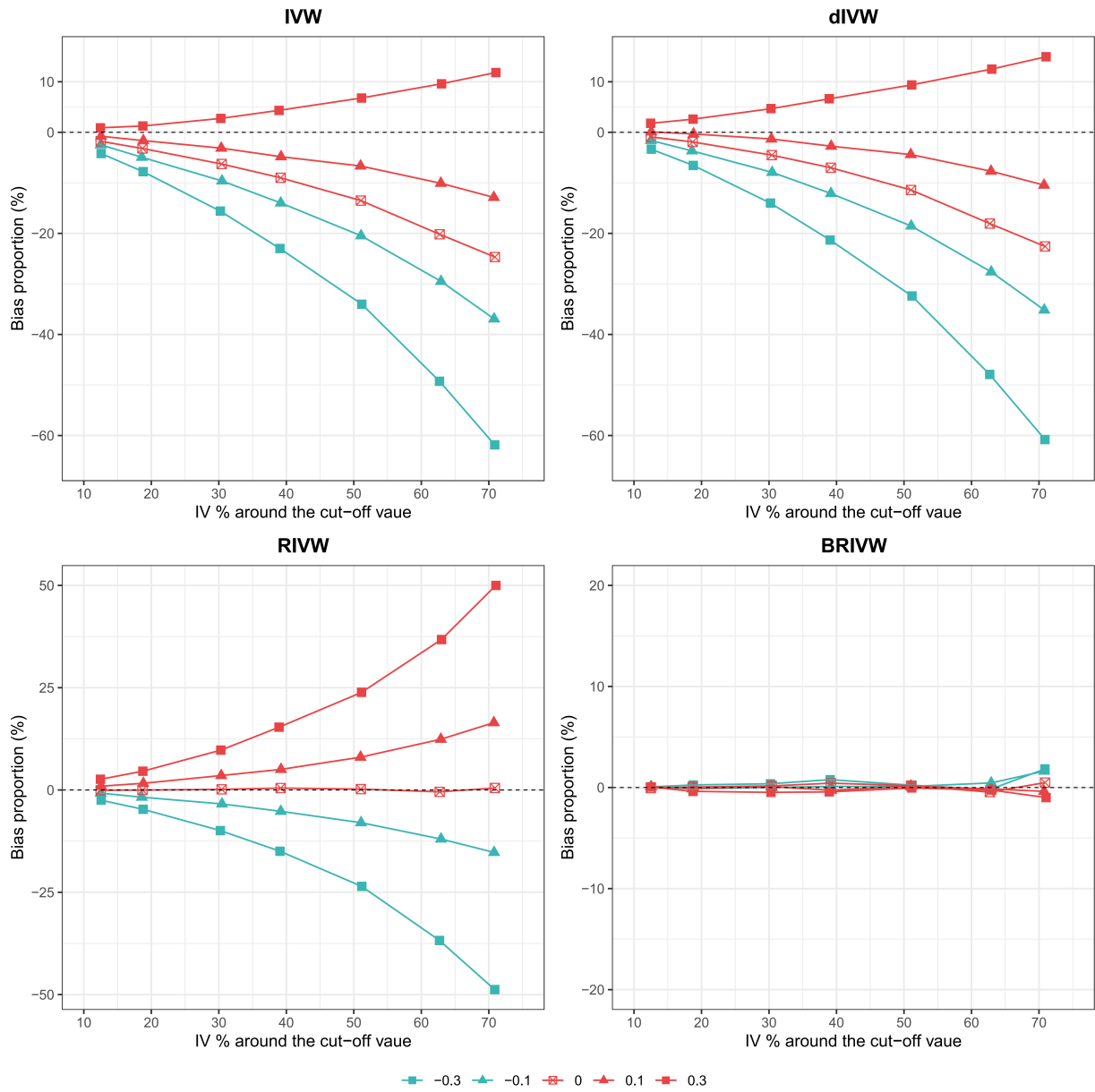


Figure 2: Bias proportion of IVW, dIVW, RIVW, and BRIVW estimators under different levels of sample structure ( $\rho$ ) and IV proportion around the selection cutoff value. The IV proportion (x-axis) is calculated as the number of IVs with p-values lying between  $5 \times 10^{-8}$  and  $5 \times 10^{-10}$  divided by the number of selected IVs with p-value  $< 5 \times 10^{-8}$ .

As the magnitude of winner's curse changes with the number of IVs around the cutoff

value  $\lambda$ , we vary  $\epsilon_x^2 = \tau^2$  in the set  $\{3 \times 10^{-5}, 4 \times 10^{-5}, 6 \times 10^{-5}, 1 \times 10^{-4}, 1.5 \times 10^{-4}, 3 \times 10^{-4}, 6 \times 10^{-4}\}$ , and  $\pi_x = \pi_y$  in the set  $\{0.002, 0.02\}$ . Some combinations are excluded because we require the heritability to lie in  $(0, 1)$ . For simplicity, we set  $\omega = 0$ , representing no pleiotropy. We set  $\lambda = \Phi^{-1}(1 - 5 \times 10^{-8}/2)$  for all methods and  $\eta = 0.5$  for RIVW and BRIVW to perform randomized IV selection. To generate GWAS summary statistics under Assumption 2, we set the sample size  $n_X = n_Y = 100,000$  and consider  $\rho$  similar to Example 1. The standard deviations are set to be  $\sigma_{\hat{\gamma}_j} = 1/\sqrt{n_X}$  and  $\sigma_{\hat{\Gamma}_j} = 1/\sqrt{n_Y}$  for all  $j$ . We report the bias proportion (Monte Carlo bias divided by the true parameter  $\beta = 0.2$ ) of IVW, dIVW, RIVW, and the proposed BRIVW estimator.

Figure 2 illustrates how weak IVs, winner’s curse, and sample structure jointly distort causal effect estimation. As the proportion of SNP–exposure associations near the selection threshold  $\lambda$  increases, selection bias intensifies, leading to increasingly distorted estimates across all methods except BRIVW. Sample structure further modulates both the magnitude and direction of this bias. Specifically, winner’s curse on the exposure side induces systematic attenuation, while winner’s curse on the outcome side generates bias whose direction depends on the sign of  $\rho$ : negative correlation amplifies downward bias, whereas positive correlation partially offsets it. As a result, IVW and dIVW exhibit pronounced asymmetry in bias with respect to  $\rho$ , with substantial underestimation when  $\rho < 0$ . In addition, IVW suffers from more severe underestimation than dIVW due to weak IV bias. BRIVW corrects weak IV bias and exposure-side selection bias, yielding bias that is symmetric in  $\rho$  and negligible when  $\rho = 0$ . In contrast, BRIVW remains approximately unbiased across all scenarios, demonstrating robustness to weak IVs, winner’s curse, and sample structure simultaneously.

## 4.2 BRIVW estimator

Although RIVW corrects for exposure-side winner’s curse, it assumes independence between SNP–exposure and SNP–outcome estimates, which is violated under sample structure and induces both outcome-side post-selection bias and additional covariance. To address these issues, we propose the BRIVW estimator, which extends RIVW by explicitly modeling the joint distribution of  $\hat{\gamma}_j$  and  $\hat{\Gamma}_j$  under sample structure. Before introducing the BRIVW

estimator, we introduce some additional notation: the number of selected IVs as  $p_\lambda = |S_\lambda|$ , and an overall measure of instrument strength after selection:

$$\kappa_\lambda = \frac{1}{p_\lambda} \sum_{j \in S_\lambda} \left( \frac{\gamma_j}{\sigma_{\hat{\gamma}_j}} \right)^2.$$

Notably, both  $p_\lambda$  and  $\kappa_\lambda$  are random variables that depend on the set of selected IVs. In addition to the assumptions in Section 2, we make the following conditions for theoretical development.

**Assumption 3.** *The cutoff value satisfies  $\lambda \rightarrow \infty$ .*

**Assumption 4.** *The true instrument effects satisfy*

$$\frac{\max_{j \in S_\lambda} \gamma_j^2}{\sum_{j \in S_\lambda} \gamma_j^2} \xrightarrow{p} 0.$$

Assumption 3 requires the cutoff value to diverge, which is well justified since  $\lambda$  is typically of the order  $\sqrt{\log p}$  to account for multiple testing. Assumption 4 stipulates that, after selection, no single instrument exerts a dominant influence. This condition rules out extreme scenarios in which the overall signal is driven by only a small number of genetic variants. We will invoke this assumption in establishing the asymptotic normality of the proposed estimator.

**Step 1** (Adjusted covariance matrix under sample structure)

Under Assumption 2, we estimate the variance correction factors  $c_1$ ,  $c_2$  and the cross-trait correlation parameter  $\rho = c_{12}/\sqrt{c_1 c_2}$  using univariate and bivariate LD score regression (LDSC; Bulik-Sullivan et al. 2015a, b). The reported GWAS standard errors are rescaled accordingly, and the resulting adjusted covariance matrix is used throughout the construction of the BRIVW estimator.

**Step 2** (Outcome-side winner’s curse removal by Rao–Blackwellization)

Recall that under sample structure,  $\text{Cov} \left( \hat{\Gamma}_j, \frac{\hat{\gamma}_j}{\sigma_{\hat{\gamma}_j}} + Z_j \right) = \rho \sigma_{\hat{\Gamma}_j}$ , so that  $\hat{\Gamma}_j$  is no longer independent of the randomized IV selection event  $j \in S_\lambda$ . To restore conditional independence, we construct the crude initial estimator,  $\hat{\Gamma}_{j,\text{ini}} = \hat{\Gamma}_j - \frac{\rho \sigma_{\hat{\Gamma}_j}}{\eta^2} Z_j$ , which is independent of  $S_j$  by construction. As a result,  $\hat{\Gamma}_{j,\text{ini}}$  is unbiased for  $\Gamma_j$  both before and after IV selection:

$$\mathbb{E}[\hat{\Gamma}_{j,\text{ini}} \mid j \in S_\lambda] = \mathbb{E}[\hat{\Gamma}_{j,\text{ini}}] = \Gamma_j.$$

Next, we apply the Rao–Blackwellization procedure to improve the efficiency of  $\hat{\Gamma}_{j,\text{ini}}$  by conditioning on the sufficient statistic:

$$\hat{\Gamma}_{j,\text{RB}} = \mathbb{E}[\hat{\Gamma}_{j,\text{ini}} \mid \hat{\Gamma}_j, \hat{\gamma}_j, j \in S_\lambda] = \hat{\Gamma}_j - \frac{\rho \sigma_{\hat{\Gamma}_j}}{\eta} \frac{\phi(A_{j,+}) - \phi(A_{j,-})}{1 - \Phi(A_{j,+}) + \Phi(A_{j,-})}.$$

**Lemma 2.** *Under Assumption 2, the Rao–Blackwellized estimator  $\hat{\Gamma}_{j,\text{RB}}$  is unbiased for the true SNP–outcome effect  $\Gamma_j$  after IV selection:*

$$\mathbb{E}[\hat{\Gamma}_{j,\text{RB}} \mid j \in S_\lambda] = \Gamma_j.$$

The unbiasedness of  $\hat{\Gamma}_{j,\text{RB}}$  after selection is a direct consequence of the law of iterated expectations and the independence between  $\hat{\Gamma}_{j,\text{ini}}$  and  $S_j$ . Thanks to the Rao–Blackwellization,  $\hat{\Gamma}_{j,\text{RB}}$  also achieves minimum variance. Notably, when  $\rho = 0$ ,  $\hat{\Gamma}_{j,\text{RB}}$  reduces to the original  $\hat{\Gamma}_j$ . The results in Figure 1 show that  $\hat{\Gamma}_{j,\text{RB}}$  is well-centered around the true value across all scenarios, confirming its effectiveness in eliminating the outcome-side winner’s curse under sample structure. Together with the exposure-side correction  $\hat{\gamma}_{j,\text{RB}}$  from RIVW, this yields a unified framework that removes the winner’s curse on both sides under sample structure.

**Step 3** (Post-selection covariance adjustment)

After obtaining the Rao–Blackwellized estimators  $\hat{\gamma}_{j,\text{RB}}$  and  $\hat{\Gamma}_{j,\text{RB}}$ , we quantify the post-selection covariance induced by sample structure. Indeed, conditional on  $j \in S_\lambda$ ,

$$\mathbb{E}\left(\hat{\Gamma}_{j,\text{RB}} \hat{\gamma}_{j,\text{RB}} \mid j \in S_\lambda\right) = \Gamma_j \gamma_j + \text{Cov}\left(\hat{\Gamma}_{j,\text{RB}}, \hat{\gamma}_{j,\text{RB}} \mid j \in S_\lambda\right),$$

so the covariance term must be accounted for when constructing the BRIVW estimator. Notably, both the selection step and the subsequent Rao–Blackwellization complicate the covariance structure. That is,  $\text{Cov}(\hat{\gamma}_{j,\text{RB}}, \hat{\Gamma}_{j,\text{RB}} \mid j \in S_\lambda) \neq \rho \sigma_{\hat{\gamma}_j} \sigma_{\hat{\Gamma}_j}$ . By the law of total covariance, we decompose

$$\sigma_{\hat{\gamma}_j \hat{\Gamma}_{j,\text{RB}}} = \left( \text{Cov}(\hat{\gamma}_{j,\text{ini}}, \hat{\Gamma}_{j,\text{ini}} \mid j \in S_\lambda) - \mathbb{E}\left[ \text{Cov}(\hat{\gamma}_{j,\text{ini}}, \hat{\Gamma}_{j,\text{ini}} \mid \hat{\Gamma}_j, \hat{\gamma}_j, j \in S_\lambda) \mid j \in S_\lambda \right] \right).$$

The first term equals the unconditional covariance, while the second term depends nonlinearly on the unknown  $\gamma_j$  and is analytically intractable. We therefore define the covariance

estimator without explicitly evaluating the outer expectation:

$$\begin{aligned}\hat{\sigma}_{\hat{\gamma}_j \hat{\Gamma}_{j,\text{RB}}} &= \text{Cov}\left(\hat{\gamma}_{j,\text{ini}}, \hat{\Gamma}_{j,\text{ini}}\right) - \text{Cov}\left(\hat{\gamma}_{j,\text{ini}}, \hat{\Gamma}_{j,\text{ini}} \mid \hat{\Gamma}_j, \hat{\gamma}_j, j \in S_\lambda\right) \\ &= \rho \sigma_{\hat{\gamma}_j} \sigma_{\hat{\Gamma}_j} \left[ 1 - \frac{1}{\eta^2} \frac{A_{j,+} \phi(A_{j,+}) - A_{j,-} \phi(A_{j,-})}{1 - \Phi(A_{j,+}) + \Phi(A_{j,-})} + \frac{1}{\eta^2} \left( \frac{\phi(A_{j,+}) - \phi(A_{j,-})}{1 - \Phi(A_{j,+}) + \Phi(A_{j,-})} \right)^2 \right].\end{aligned}\quad (4)$$

This estimator is unbiased for the true post-selection covariance conditional on  $j \in S_\lambda$ , but is generally inconsistent. Nevertheless, the BRIVW estimator only requires accurate estimation of the aggregated covariance  $\sum_{j \in S_\lambda} \hat{\sigma}_{\hat{\gamma}_j \hat{\Gamma}_{j,\text{RB}}}$ , as formalized below.

**Lemma 3.** *Under Assumption 2 and 3, we have  $\mathbb{E}\left[\hat{\sigma}_{\hat{\gamma}_j \hat{\Gamma}_{j,\text{RB}}} \mid j \in S_\lambda\right] = \sigma_{\hat{\gamma}_j \hat{\Gamma}_{j,\text{RB}}}$ , and*

$$\left| \sum_{j \in S_\lambda} \left( \hat{\sigma}_{\hat{\gamma}_j \hat{\Gamma}_{j,\text{RB}}} - \sigma_{\hat{\gamma}_j \hat{\Gamma}_{j,\text{RB}}} \right) \right| = O_p(v^2 \lambda \sqrt{p_\lambda}).$$

**Remark.** Lemma 3 implies that the aggregated covariance correction is estimable up to a remainder of order  $O_p(v^2 \lambda \sqrt{p_\lambda})$ , which is asymptotically negligible relative to the leading term  $\sum_{j \in S_\lambda} \sigma_{\hat{\gamma}_j \hat{\Gamma}_{j,\text{RB}}} = O_p(p_\lambda v^2)$  (See Appendix S4).

Similarly, correcting weak-IV bias requires estimating the variance of  $\hat{\gamma}_{j,\text{RB}}$ . Following Ma et al. (2023), we use

$$\hat{\sigma}_{\hat{\gamma}_{j,\text{RB}}}^2 = \sigma_{\hat{\gamma}_j}^2 \left[ 1 - \frac{1}{\eta^2} \frac{A_{j,+} \phi(A_{j,+}) - A_{j,-} \phi(A_{j,-})}{1 - \Phi(A_{j,+}) + \Phi(A_{j,-})} + \frac{1}{\eta^2} \left( \frac{\phi(A_{j,+}) - \phi(A_{j,-})}{1 - \Phi(A_{j,+}) + \Phi(A_{j,-})} \right)^2 \right], \quad (5)$$

for which the aggregated variance  $\sum_{j \in S_\lambda} \hat{\sigma}_{\hat{\gamma}_{j,\text{RB}}}^2$  is also estimable with a negligible remainder (see Appendix S4).

#### Step 4 (BRIVW estimation and inference)

Combining Steps 1–3, we define the BRIVW estimator by

$$\hat{\beta}_{\text{BRIVW}} = \frac{\sum_{j \in S_\lambda} (\hat{\Gamma}_{j,\text{RB}} \hat{\gamma}_{j,\text{RB}} - \hat{\sigma}_{\hat{\gamma}_j \hat{\Gamma}_{j,\text{RB}}}) \sigma_{\hat{\Gamma}_j}^{-2}}{\sum_{j \in S_\lambda} (\hat{\gamma}_{j,\text{RB}}^2 - \hat{\sigma}_{\hat{\gamma}_{j,\text{RB}}}^2) \sigma_{\hat{\Gamma}_j}^{-2}}. \quad (6)$$

Compared with the classical IVW estimator, BRIVW jointly corrects for winner’s curse on both exposure and outcome sides, sample-structure-induced covariance, and weak IV bias, while retaining a closed-form IVW-type estimator. When  $\rho = 0$  and  $c_1 = c_2 = 1$ , BRIVW reduces to RIVW, and thus can be viewed as its natural extension under sample structure.

Because our BRIVW estimator resembles the “slope coefficient” obtained from regressing  $\hat{\Gamma}_{j,\text{RB}}$  on  $\hat{\gamma}_{j,\text{RB}}$ , the proposed variance estimator can be motivated from the use of “regression residuals”:

$$\hat{V}_{\text{BRIVW}} = \frac{\sum_{j \in S_\lambda} [\hat{\Gamma}_{j,\text{RB}} \hat{\gamma}_{j,\text{RB}} - \hat{\sigma}_{\hat{\gamma}_j \hat{\Gamma}_j, \text{RB}} - \hat{\beta}_{\text{BRIVW}} (\hat{\gamma}_{j,\text{RB}}^2 - \hat{\sigma}_{\hat{\gamma}_j, \text{RB}}^2)]^2 / \sigma_{\hat{\Gamma}_j}^4}{\left[ \sum_{j \in S_\lambda} (\hat{\gamma}_{j,\text{RB}}^2 - \hat{\sigma}_{\hat{\gamma}_j, \text{RB}}^2) / \sigma_{\hat{\Gamma}_j}^2 \right]^2}. \quad (7)$$

Then a two-sided  $100(1 - \alpha)\%$  two-sided confidence interval (CI) for  $\beta$  can be constructed as

$$\left[ \hat{\beta}_{\text{BRIVW}} - \Phi^{-1}(1 - \alpha/2) \sqrt{\hat{V}_{\text{BRIVW}}}, \hat{\beta}_{\text{BRIVW}} + \Phi^{-1}(1 - \alpha/2) \sqrt{\hat{V}_{\text{BRIVW}}} \right].$$

**Theoretical guarantees.** We next summarize the large-sample properties of  $\hat{\beta}_{\text{BRIVW}}$  and  $\hat{V}_{\text{BRIVW}}$ ; proofs are deferred to the Appendix.

**Theorem 1.** *Assume that Assumptions 2–3 hold,  $p_\lambda \rightarrow \infty$ , and  $\kappa_\lambda / \lambda^2 \rightarrow \infty$ . Then, conditional on the selected IV set  $S_\lambda$ , we have*

$$\hat{\beta}_{\text{BRIVW}} \xrightarrow{p} \beta.$$

Moreover, if Assumption 4 additionally holds, then

$$V_{\text{BRIVW}}^{-1/2} (\hat{\beta}_{\text{BRIVW}} - \beta) \xrightarrow{d} N(0, 1),$$

where

$$V_{\text{BRIVW}} = \frac{\text{Var} \left[ \sum_{j \in S_\lambda} u_{j,\text{BRIVW}} / \sigma_{\hat{\Gamma}_j}^2 \mid S_\lambda \right]}{\left( \sum_{j \in S_\lambda} \gamma_j^2 / \sigma_{\hat{\Gamma}_j}^2 \right)^2} = O_p \left( \frac{1}{p_\lambda \kappa_\lambda} \right),$$

$$u_{j,\text{BRIVW}} = \gamma_j (u_{\hat{\Gamma}_j, \text{RB}} - \beta u_{\hat{\gamma}_j, \text{RB}}) + \left( (u_{\hat{\gamma}_j, \text{RB}} u_{\hat{\Gamma}_j, \text{RB}} - \hat{\sigma}_{\hat{\gamma}_j \hat{\Gamma}_j, \text{RB}}) - \beta (u_{\hat{\gamma}_j, \text{RB}}^2 - \hat{\sigma}_{\hat{\gamma}_j, \text{RB}}^2) \right),$$

$$u_{\hat{\gamma}_j, \text{RB}} = \hat{\gamma}_{j,\text{RB}} - \gamma_j, \quad u_{\hat{\Gamma}_j, \text{RB}} = \hat{\Gamma}_{j,\text{RB}} - \Gamma_j.$$

**Theorem 2.** *Assume Assumptions 2–4 hold,  $p_\lambda \rightarrow \infty$ , and  $\kappa_\lambda / \lambda^2 \rightarrow \infty$ . Then*

$$\frac{\hat{V}_{\text{BRIVW}}}{V_{\text{BRIVW}}} \xrightarrow{p} 1.$$

To demonstrate the intuition behind Theorem 1, we rewrite the BRIVW estimator as

$$\hat{\beta}_{\text{BRIVW}} = \beta + \frac{\sum_{j \in S_\lambda} u_{j,\text{BRIVW}} / \sigma_{\hat{\Gamma}_j}^2}{\sum_{j \in S_\lambda} (\hat{\gamma}_{j,\text{RB}}^2 - \hat{\sigma}_{\hat{\gamma}_j, \text{RB}}^2) / \sigma_{\hat{\Gamma}_j}^2}.$$

Lemmas 2 and 3 imply  $\mathbb{E}[u_{j,\text{BRIVW}} \mid j \in S_\lambda] = 0$ , ensuring asymptotic unbiasedness after IV selection. Together with the convergence of the denominator, this representation establishes Theorem 1 and motivates the residual-based variance estimator. Theorem 2 further guarantees the consistency of  $\widehat{V}_{\text{BRIVW}}$ .

**Step 5** (Extension to account for balanced pleiotropy)

We now extend the BRIVW estimator to a common pleiotropy setting known as balanced pleiotropy. In this scenario, the linear structural model for SNP–outcome effects is modified to

$$Y = \beta X + \sum_{j=1}^p \alpha_j G_j + \beta_{UY} U + E_Y, \quad (8)$$

where the pleiotropic effects  $\alpha_1, \alpha_2, \dots, \alpha_p$  are mutually independent, have mean zero and variance  $\tau^2$ , and are independent of  $X$ ,  $G_j$ 's,  $U$ ,  $E_X$ , and  $E_Y$ . To incorporate balanced pleiotropy, we rewrite Assumption 2 as follows.

**Assumption 2'**. *Assumption 2 holds except that the distribution of  $(\hat{\gamma}_j, \hat{\Gamma}_j)$  is modified to*

$$\begin{bmatrix} \hat{\gamma}_j \\ \hat{\Gamma}_j \end{bmatrix} \sim N \left( \begin{bmatrix} \gamma_j \\ \beta \gamma_j + \alpha_j \end{bmatrix}, \begin{bmatrix} \sigma_{\hat{\gamma}_j}^2 & \rho \sigma_{\hat{\gamma}_j} \sigma_{\hat{\Gamma}_j} \\ \rho \sigma_{\hat{\gamma}_j} \sigma_{\hat{\Gamma}_j} & \sigma_{\hat{\Gamma}_j}^2 \end{bmatrix} \right),$$

*In addition,  $\tau/v$  is bounded.*

Under Assumption 2', the winner's curse correction steps in BRIVW remain unchanged, as they do not depend on the pleiotropic effects  $\alpha_j$ . Because the pleiotropic effects are centered with mean zero, they do not introduce additional bias into the BRIVW point estimator. Although the presence of pleiotropy inflates the variability of the estimates, the residual-based variance estimator in Equation (7), constructed in the same spirit as in Ma et al. (2023), remains valid, and its functional form is unchanged. Consequently, practitioners do not need to modify either the point estimator or the variance formula when balanced pleiotropy is present, which simplifies practical implementation. Moreover, balanced pleiotropy can be viewed as a sufficient condition for the InSIDE assumption. By explicitly correcting spurious associations induced by sample structure, the BRIVW framework makes the InSIDE assumption more plausible in practice.

## 5 Simulation studies

### 5.1 Simulation settings

In this section, we conduct extensive simulation studies to evaluate the performance of the proposed BRIVW estimator compared to nine summary-level MR methods, including IVW (Didelez and Sheehan 2007), RIVW (Ma, Wang, and Wu 2023), Egger (Bowden, Davey Smith, and Burgess 2015), RAPS (Zhao et al. 2020), Weighted-median (Bowden et al. 2016), Weighted-mode (Hartwig, Davey Smith, and Bowden 2017), ConMix (Burgess et al. 2020), MRMix (Qi and Chatterjee 2019), and MR-APSS (Hu et al. 2022). We adopt the simulation setup described in Example 2. In particular, we set  $\omega = 0$ ,  $\pi_x = 0.02$ ,  $\pi_y = 0.01$ , and  $\epsilon_x^2 = \tau^2 = 5 \times 10^{-5}$  to generate SNP effects. The true causal effect is set to  $\beta \in \{-0.2, -0.1, -0.05, 0, 0.05, 0.1, 0.2\}$ . Because some MR methods are computationally intensive, we simulate 500 Monte Carlo samples under  $\beta \neq 0$  and 1,000 Monte Carlo samples under  $\beta = 0$  to evaluate power and type I error, respectively.

Following common practice, we set the IV selection threshold to  $\lambda = \Phi^{-1}(1 - 5 \times 10^{-8}/2)$  (genome-wide significance level) for IVW, Egger, RAPS, Weighted-median, Weighted-mode, ConMix, and MRMix. For MR-APSS, we use its default setting of  $\lambda = \Phi^{-1}(1 - 5 \times 10^{-5}/2)$ . Sensitivity analyses on  $\lambda$  and the randomization parameter  $\eta$  for BRIVW are reported in Appendix S5, where BRIVW is shown to be stable across a wide range of tuning choices. In practice, we recommend a more liberal threshold  $\lambda = \Phi^{-1}(1 - 5 \times 10^{-5}/2)$  with  $\eta = 0.5$  to improve efficiency, consistent with the default setting of RIVW.

We report our simulation results with five measures: “Type I error” (the proportion of times the null hypothesis is rejected when  $\beta = 0$ ), “Power” (the proportion of times the null hypothesis is rejected when  $\beta \neq 0$ ), “Bias” (the average estimation error  $\hat{\beta} - \beta$ ), “MSE” (the mean squared error, i.e., the average squared difference between the estimated  $\hat{\beta}$  and  $\beta$ ), and “Coverage” (the empirical coverage probability of the two-sided 95% CI). The simulation results under various scenarios are summarized in Figures 3.

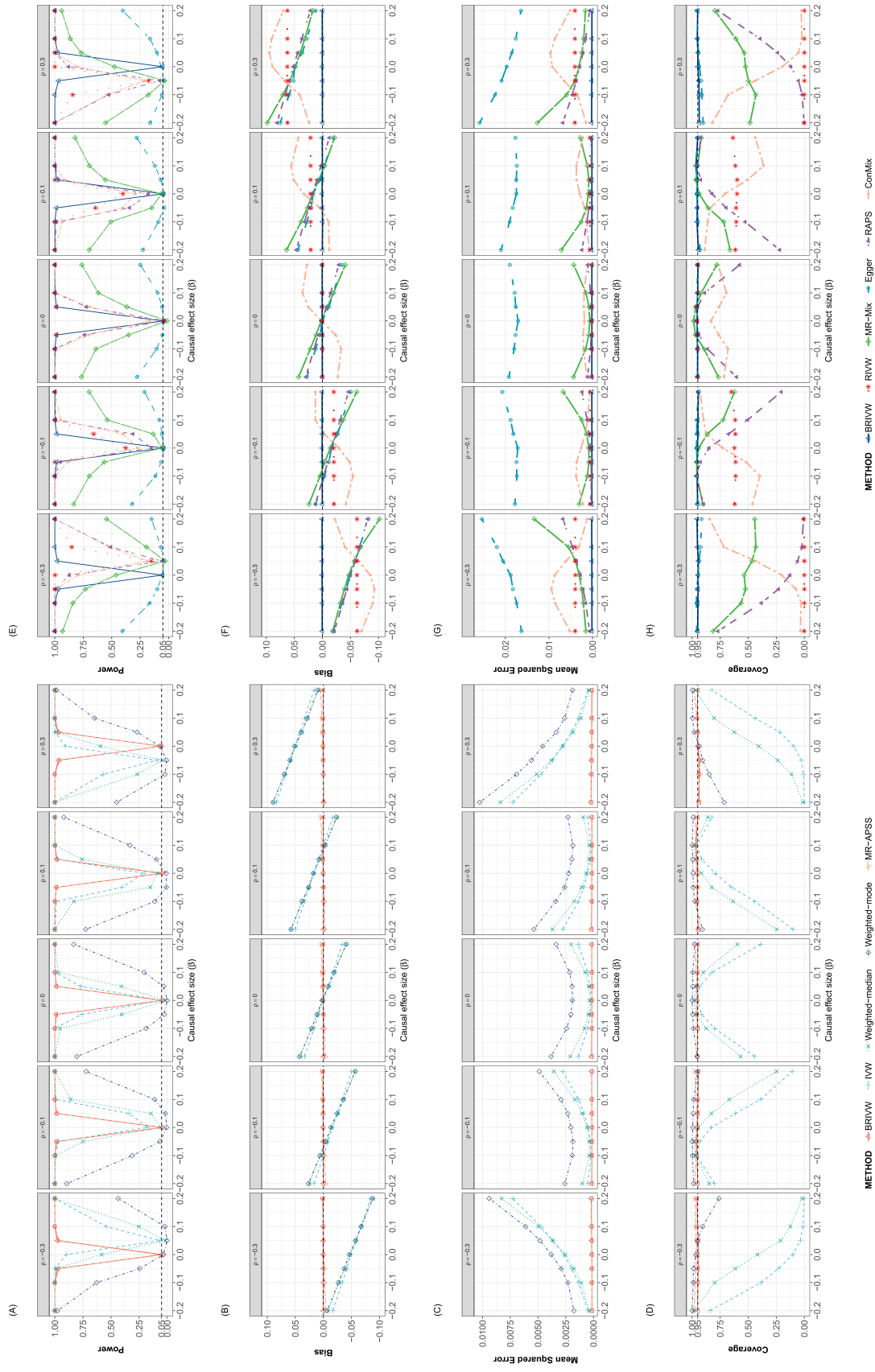


Figure 3: Power, bias, MSE, and coverage of the BRIW estimator and several robust MR methods under the no horizontal pleiotropy setting with  $\omega = 0$ .

## 5.2 Simulation results

Figures 3A and 3E present the type I error rates ( $\beta = 0$ ) and power ( $\beta \neq 0$ ) of different methods under varying degrees of sample structure ( $\rho \in \{-0.3, -0.1, 0, 0.1, 0.3\}$ ). When there is no sample structure ( $\rho = 0$ ), all methods control type I error near the nominal 0.05 level. However, under the sample structure ( $\rho \neq 0$ ), IVW, RIVW, RAPS, Weighted-median, ConMix, and MRMix exhibit inflated type I error rates, with the degree of inflation increasing with  $|\rho|$ . By contrast, BRIVW, Egger, Weighted-mode, and MR-APSS maintain well-controlled type I error across all scenarios. Among methods with controlled type I error, BRIVW consistently achieves the highest power. Figures 3B and 3F display the bias of different methods. All competing methods, except MR-APSS, exhibit substantial bias arising from the combined effects of weak IVs, the winner’s curse, and sample structure. Weak IV bias and the exposure-side winner’s curse systematically shrink causal estimates toward zero. In contrast, spurious associations induced by sample structure, together with the outcome-side winner’s curse, push estimates away from zero in the direction determined by  $\rho$ . As a result, these biases partially offset when  $\rho$  and  $\beta$  share the same sign but reinforce each other when their signs differ, leading to either attenuated or exaggerated bias across scenarios. By explicitly correcting all three sources of bias, BRIVW remains approximately unbiased across all settings. We observe similar patterns in MSE (Figures 3C and 3G) and coverage probability (Figures 3D and 3H). BRIVW uniformly achieves the lowest MSE and nominal 95% coverage, whereas competing methods suffer from inflated MSE and poor coverage. Egger and Weighted Mode attain nominal coverage only due to conservative standard errors, but their substantial bias leads to inferior MSE performance.

Under the normal mixture settings considered here, MR-APSS performs comparably to BRIVW. However, additional simulations reported in the Appendix S5 show that, when the mixture distribution includes both normal and uniform components, MR-APSS exhibits increased bias, higher MSE, and deteriorated coverage, whereas BRIVW continues to perform well. Moreover, MR-APSS incurs substantially higher computational costs (See Appendix S5). These results suggest that MR-APSS is sensitive to model misspecification and computationally intensive, while BRIVW is both more robust and more efficient. We further conduct additional simulations under a broader range of settings, including bal-

anced pleiotropy and unequal sample sizes for the exposure and outcome GWAS. As shown in the Appendix S5, BRIVW continues to deliver accurate causal effect estimation and valid statistical inference across these scenarios, highlighting its robustness and practical utility in Mendelian randomization analyses.

## 6 Real data analysis

We apply the proposed BRIVW method to real GWAS summary statistics to evaluate its empirical performance from three complementary perspectives: (i) negative control outcome analyses to assess type I error control; (ii) same-trait analyses to examine the accuracy of causal effect estimation; and (iii) causal inference among complex traits to evaluate power in detecting true causal effects.

### 6.1 Data processing

The GWAS summary statistics are processed in three steps: quality control, data harmonization and estimation of sample structure, and IV selection. First, we apply the quality control procedures described in MR-APSS (Hu et al. 2022); details are provided in the Appendix S6. Second, exposure and outcome summary statistics are harmonized to ensure consistent effect-allele alignment, after which the sample structure parameters ( $c_1, c_2, c_{12}$ ) are estimated using LDSC. Finally, independent IVs are selected using the revised sigma-based pruning procedure proposed in RIVW (Ma, Wang, and Wu 2023), retaining SNPs with pairwise LD  $R^2 < 0.001$  within a 10,000 Kb window. Unlike conventional  $p$ -value-based clumping, this approach preferentially retains variants with smaller standard errors for the SNP-exposure association, thereby mitigating additional selection bias (Robertson, Prevost, and Bowden 2016) while preserving estimation efficiency. For BRIVW and RIVW, we adopt the default tuning parameters  $\lambda = \Phi^{-1}(1 - 5 \times 10^{-5}/2)$  and  $\eta = 0.5$ . For MR-APSS, we use  $\lambda = \Phi^{-1}(1 - 5 \times 10^{-5}/2)$ , while a more stringent genome-wide threshold  $\lambda = \Phi^{-1}(1 - 5 \times 10^{-8}/2)$  is applied to the remaining competing methods.

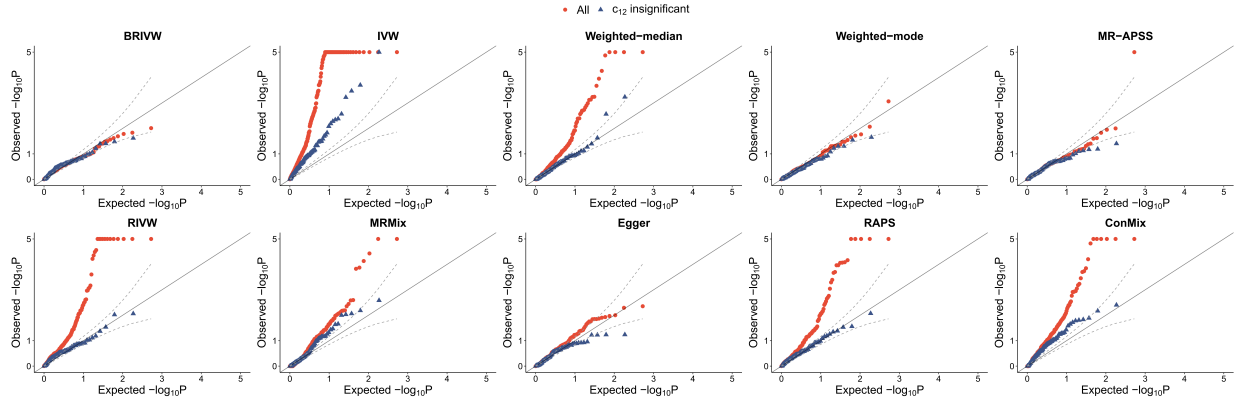


Figure 4: Quantile-quantile plots of  $-\log_{10}(p)$  from different MR methods across 265 exposure–outcome pairs in the negative control outcome analysis. The red dots represent all 265 pairs, while the blue triangles represent the 93 pairs with insignificant  $c_{12}$  values. The black diagonal line indicates the expected distribution under the null hypothesis.

## 6.2 Negative control outcome analysis

To fairly assess the type I error control of different MR methods in real data, we use the negative control outcomes proposed by Sanderson et al. (2021), where sample structure is likely present but no causal effect is expected. Specifically, we select 5 negative control outcomes from the UK Biobank data, including natural hair color before graying (Black, Blonde, Light Brown, Dark Brown) and skin tanning ability (Tanning). A total of 61 exposure traits are drawn from the UK Biobank, the Genomic Consortium, and other large-scale GWAS consortia, covering anthropometric, cardiovascular, immune-related, neuropsychiatric, lifestyle, and disease traits (see Appendix S6). We apply BRIVW and nine competing MR methods to all exposure–outcome combinations, yielding 305 pairs. Due to stringent IV selection ( $P < 5 \times 10^{-8}$ ), some exposure–outcome pairs contain very few or no valid IVs, precluding the application of certain methods. To ensure a fair comparison, we restrict attention to 265 exposure–outcome pairs with at least four IVs available for all methods.

Figure 4 displays the quantile-quantile (QQ) plots of the  $-\log_{10}(p)$  from different MR methods across the 265 exposure–outcome pairs (red dots). BRIVW produces well-calibrated  $P$  values closely following the null expectation, demonstrating effective type I error control. Weighted-mode and MR-APSS also achieve good performance, although MR-APSS shows slight inflation in the tail area. In contrast, IVW, RIVW, RAPS, Weighted-

median, ConMix, and MRMix produce overly inflated  $P$  values, while Egger produces slightly inflated  $P$  values. To explore the source of this inflation, we examined the estimated sample structure correlation parameter  $c_{12}$  for each exposure–outcome pair (Appendix S6). Of the 265 pairs, 172 (64.9%) showed significant nonzero  $c_{12}$  values (\*,  $p < 0.05$ ), indicating that sample structure is widespread in real GWAS data. We restricted the QQ plot analysis to the 93 exposure–outcome pairs with insignificant  $c_{12}$  values (blue triangles in Figure 4A). In this subset,  $P$  values are substantially better calibrated for all methods except IVW, suggesting that unaccounted sample structure is the primary driver of inflated type I error rates in conventional MR methods. We also conduct additional negative control outcome analyses employing standard LD clumping, as shown in the Appendix S6. Under this common strategy, most methods produce even more inflated  $P$  values, indicating that traditional p-value-based clumping can exacerbate type I error inflation due to additional selection bias. Egger and Weighted-mode remain well calibrated due to their conservative standard errors. These results suggest that the revised sigma-based pruning procedure may help mitigate additional selection bias in practice.

### 6.3 Same trait analyses

In this section, we use two separate GWAS summary datasets for the same trait as the exposure and outcome. Under this same-trait design, the true causal effect is 1, providing a direct benchmark for assessing the accuracy of BRIVW relative to competing methods. We consider two same traits analyses: (i) body mass index (BMI) with GWAS summary statistics from the UK Biobank [sample size: 461,460, ID: ukb-b-19953] (Bycroft et al. 2018) and the GIANT consortium [sample size: 339,224, ID: ieu-a-2] (Locke et al. 2015), denoted by BMI-1 and BMI-2, respectively; (ii) high-density lipoprotein (HDL) with GWAS summary statistics from the UK Biobank [sample size: 403,943, ID: ukb-b-109] (Bycroft et al. 2018) and the Global Lipids Genetics Consortium [sample size: 94,595, ID: ebi-a-GCST002223] (Willer et al. 2013), denoted by HDL-1 and HDL-2, respectively. For each trait, analyses are conducted in both directions, yielding four exposure–outcome configurations. Figure 5 reports the estimated causal effects and two-sided 95% CIs from different MR methods.

Across all four dataset configurations, BRIVW yields estimates close to the true effect

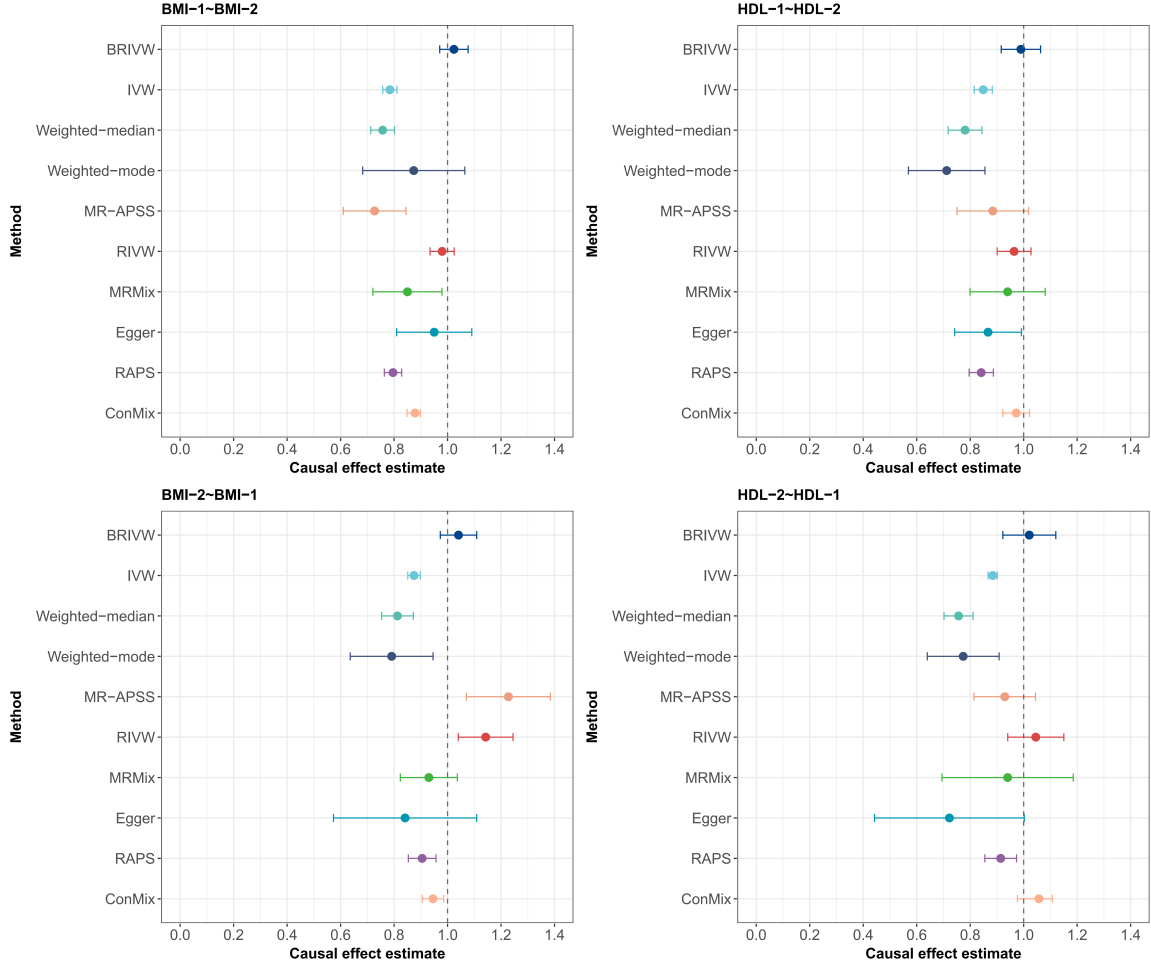


Figure 5: Same trait results for different methods under the revised sigma-based pruning procedure

( $\beta = 1$ ) with narrow 95% CIs, indicating high accuracy and efficiency. By contrast, most competing methods systematically underestimate the causal effect, reflecting the dominant influence of weak IV bias and the exposure-side winner’s curse, which shrink estimates toward zero. Notably, RIVW and MR-APSS exhibit a distinct pattern, occasionally overestimating the causal effect. To explain this, we examine the estimated sample structure parameters ( $c_1$ ,  $c_2$ , and  $c_{12}$ ; Appendix S6). Although the two GWAS datasets are derived from independent studies, both  $c_1$  and  $c_2$  deviate substantially from 1, indicating pronounced population stratification and resulting in a positive  $c_{12}$ . For methods that do not adequately correct weak IV bias and exposure-side winner’s curse, the downward bias toward zero dominates, and the upward bias induced by positive sample structure is insuf-

ficient to offset this shrinkage, leading to systematic underestimation. In contrast, RIVW and MR-APSS partially mitigate these shrinkage effects, allowing the inflation induced by positive sample structure to manifest in some configurations (e.g., BMI-2  $\rightarrow$  BMI-1), leading to overestimation. Supplementary results based on standard LD clumping are provided in the Appendix S6. Except for MR-APSS, which overestimates the effect in the BMI-2  $\rightarrow$  BMI-1 configuration, all other methods consistently attenuate the causal estimate, further suggesting that  $P$ -value-driven clumping can introduce additional selection bias.

## 6.4 Causal relationships among complex traits

Cardiometabolic diseases (CMDs), particularly coronary artery disease (CAD), type 2 diabetes (T2D), and stroke, impose a substantial public health burden, and their frequent co-occurrence in aging populations is associated with marked reductions in life expectancy, underscoring the need to identify upstream causal risk factors (Di Angelantonio et al. 2015; Jin et al. 2023; Zhao et al. 2024). We further compare our proposed BRIVW with other methods to identify possible causal effects of 52 complex traits on these three cardiometabolic diseases (CAD, T2D, and stroke). The 52 exposure traits are the same as those used in the negative control outcome analysis, while the outcome GWAS summary statistics are obtained from large-scale consortia (see Appendix S6). In total, 156 exposure-outcome pairs were considered; after excluding four pairs with fewer than four instrumental variables under stringent IV selection ( $P < 5 \times 10^{-8}$ ), 152 pairs were retained for analysis.

We first examined the estimated sample structure correlation parameter  $c_{12}$  for each exposure-outcome pair (Appendix). Among the 152 pairs, 67 exhibited significant nonzero  $c_{12}$  at the 0.05 level, and 32 remained significant after Bonferroni correction, indicating that sample structure is prevalent in real GWAS data and may confound MR analyses if unaccounted for. We then compared the number of significant causal effects detected by BRIVW and competing methods under Bonferroni correction ( $< 0.05/152 \approx 0.0003$ ; Figure 6A). BRIVW identified 26 significant associations, exceeding most competitors, including MRMix (21), MR-APSS (11), Weighted-mode (5), and Egger (4). Although IVW (55), RAPS (37), RIVW (33), ConMix (33), and Weighted-median (28) reported more signals, our negative control analysis indicates that their type I error is inflated

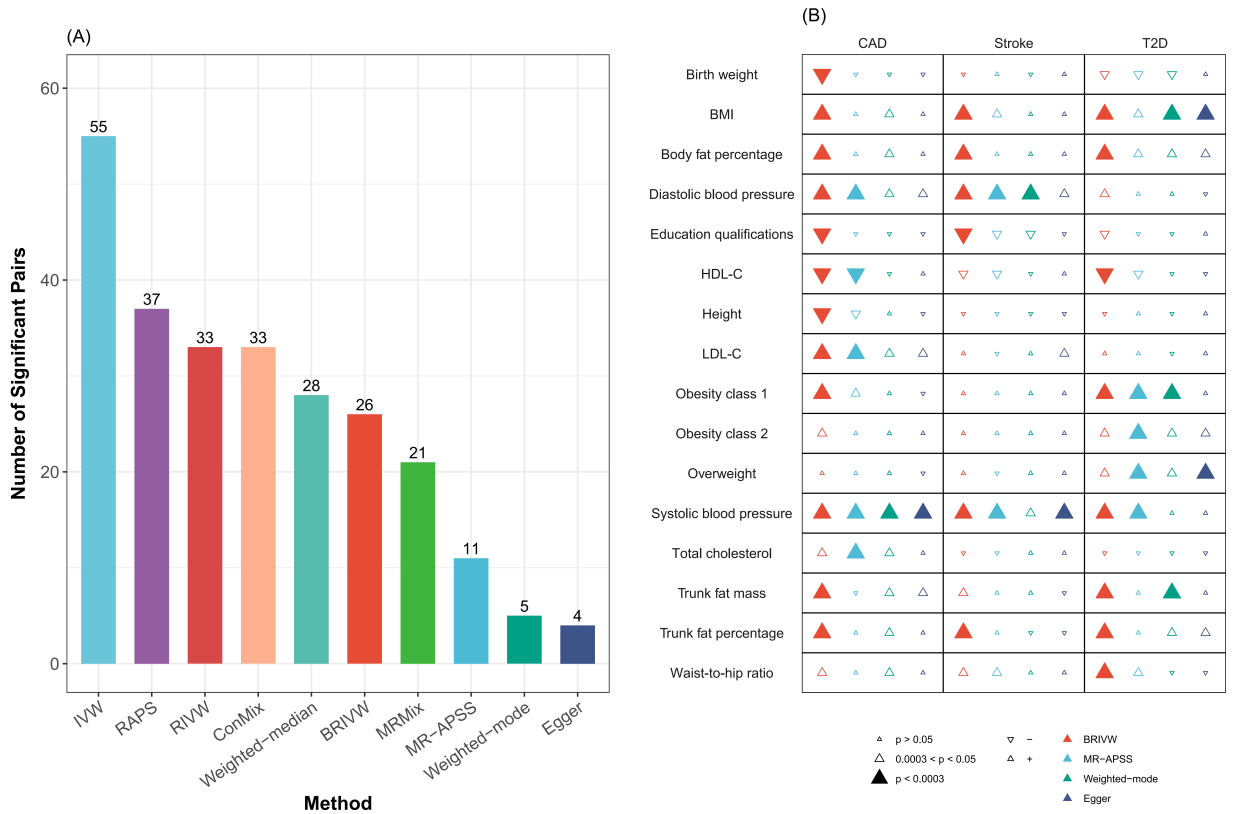


Figure 6: Results of causal relationships among complex traits. (A) Number of significant causal effects detected by different methods under Bonferroni correction ( $< 0.05/152 \approx 0.0003$ ). (B) Significant causal effects identified by BRIVW, MR-APSS, Weighted-mode, and Egger under Bonferroni correction.

when sample structure is unaccounted for. We therefore focus subsequent comparisons on methods with well-calibrated type I error: BRIVW, MR-APSS, Weighted-mode, and Egger (Figure 6B). Overall, the four methods converge on several key patterns: adiposity- and blood pressure-related traits (especially systolic blood pressure) consistently show risk-increasing effects on cardiometabolic outcomes, whereas education qualifications tend to be protective. Notably, BRIVW identifies more Bonferroni-significant associations than MR-APSS, Weighted-mode, and Egger, including several biologically plausible risk factors supported by prior literature. For example, only BRIVW finds that trunk fat percentage has a positive causal effect on CAD, stroke, and T2D. This is in line with evidence that links central adiposity to cardiometabolic risk (Neeland et al. 2012; Emdin et al. 2017). Together, these findings indicate that, under proper calibration, BRIVW delivers higher

power in real data and more effectively identifies plausible causal risk factors.

## 7 Discussion

In this article, we propose the BRIVW estimator that simultaneously corrects for weak IV bias, winner’s curse, and sample structure in two-sample summary-data MR analyses. Extensive simulations and real data analyses confirmed that BRIVW effectively controls type I error rates, yields accurate causal effect estimates, and achieves higher power compared to existing methods. Notably, RIVW (Ma, Wang, and Wu 2023) can be viewed as a special case of BRIVW when there is no sample structure (i.e.,  $c_{12} = 0$ , and  $c_1 = c_2 = 1$ ). When sample structure is present, however, RIVW may yield severely biased estimates and inflated type I error rates, as it does not account for the induced correlation between SNP–exposure and SNP–outcome association estimates. Our results clarify that this correlation not only propagates exposure-side winner’s curse to the outcome side but also generates spurious associations, thereby amplifying false-positive findings. By contrast, BRIVW applies Rao–Blackwellization to both exposure and outcome associations and explicitly accounts for their post-selection covariance, jointly correcting weak IV bias, two-sided winner’s curse, and sample structure. Following MR-APSS (Hu et al. 2022), we estimate the sample-structure parameters using LDSC. Unlike the likelihood-based MR-APSS, which relies on additional distributional assumptions, BRIVW retains a closed-form IVW-type solution, offering computational efficiency and increased robustness to model misspecification. Moreover, BRIVW can be readily extended to accommodate balanced horizontal pleiotropy without modifying the estimator’s form, which simplifies implementation in practice. Therefore, we recommend BRIVW as a robust and efficient tool for MR analyses using GWAS summary data.

From an applied perspective, BRIVW permits more flexible IV selection thresholds, allowing the inclusion of moderately associated variants. This feature is particularly advantageous for highly polygenic traits, such as many psychiatric disorders (Sullivan et al. 2018), for which genome-wide significant instruments are often scarce. In addition, BRIVW reduces the need to restrict analyses to homogeneous or non-overlapping GWAS datasets, allowing investigators to leverage large consortia data that may involve residual population

stratification or sample overlap. The method also encourages routine reporting of LDSC-based diagnostics ( $c_1$ ,  $c_2$ , and  $c_{12}$ ) and sensitivity analyses across selection thresholds. In practice, sigma-based pruning is preferable to standard LD clumping to mitigate additional selection bias.

Several limitations warrant further investigation. BRIVW relies on LDSC to estimate sample-structure parameters, and its performance may depend on the validity of LDSC assumptions. Future work could develop alternative estimators of sample structure or procedures that are less sensitive to LDSC inputs. Additionally, although BRIVW corrects balanced pleiotropy, it does not currently address directional or correlated pleiotropy. Extending the BRIVW correction framework to MR estimators that are robust to these forms of horizontal pleiotropy, or developing dedicated sensitivity tests, remains an important direction for future research.

## Acknowledgements

## References

- Bondemark, L., and Ruf, S. (2015). Randomized controlled trial: The gold standard or an unobtainable fallacy? *European Journal of Orthodontics* 37(5), 457–461. doi: 10.1093/ejo/cjv046.
- Bowden, J., Davey Smith, G., and Burgess, S. (2015). Mendelian randomization with invalid instruments: Effect estimation and bias detection through Egger regression. *International Journal of Epidemiology* 44(2), 512–525. doi: 10.1093/ije/dyv080.
- Bowden, J., Davey Smith, G., Haycock, P. C., and Burgess, S. (2016). Consistent estimation in Mendelian randomization with some invalid instruments using a weighted median estimator. *Genetic Epidemiology* 40(4), 304–314. doi: 10.1002/gepi.21965.
- Bowden, J., Del Greco M, F., Minelli, C., Davey Smith, G., Sheehan, N., and Thompson, J. (2017). A framework for the investigation of pleiotropy in two-sample sum-

- mary data Mendelian randomization. *Statistics in Medicine* 36(11), 1783–1802. doi: 10.1002/sim.7221.
- Bulik-Sullivan, B., Loh, P.R., Finucane, H. et al. (2015a). LD Score regression distinguishes confounding from polygenicity in genome-wide association studies. *Nature Genetics* 47(3), 291–295. doi: 10.1038/ng.3211.
- Bulik-Sullivan B, Finucane H K, Anttila V, et al. (2015b). An atlas of genetic correlations across human diseases and traits. *Nature Genetics* 47(11), 1236–1241. doi: 10.1038/ng.3406.
- Burgess, S., Butterworth, A., Malarstig, A., and Thompson, S. G. (2012). Use of Mendelian randomisation to assess potential benefit of clinical intervention. *British Medical Journal* 345, e7325. doi: 10.1136/bmj.e7325.
- Burgess, S., Scott, R.A., Timpson, N.J. et al. (2015). Using published data in Mendelian randomization: A blueprint for efficient identification of causal risk factors. *European Journal of Epidemiology* 30(7), 543–552. doi: 10.1007/s10654-015-0011-z.
- Burgess, S., Davies, N. M., and Thompson, S. G. (2016). Bias due to participant overlap in two-sample Mendelian randomization. *Genetic Epidemiology* 40(7), 597–608. doi: 10.1002/gepi.21998.
- Burgess, S., Small, D. S., and Thompson, S. G. (2017). A review of instrumental variable estimators for Mendelian randomization. *Statistical Methods in Medical Research* 26(5), 2333–2355. doi: 10.1177/0962280215597579.
- Burgess, S., Foley, C. N., Allara, E., Staley, J. R., and Howson, J. M. (2020). A robust and efficient method for Mendelian randomization with hundreds of genetic variants. *Nature Communications* 11(1), 376. doi: 10.1038/s41467-019-14156-4.
- Bycroft, C., Freeman, C., Petkova, D., Band, G., Elliott, L. T., Sharp, K., Motyer, A., Vukcevic, D., Delaneau, O., O’Connell, J., Cortes, A., Welsh, S., Young, A., Effingham, M., McVean, G., Leslie, S., Allen, N., Donnelly, P., and Marchini, J. (2018). The UK

- Biobank resource with deep phenotyping and genomic data. *Nature* 562(7726), 203–209. doi: 10.1038/s41586-018-0579-z.
- Di Angelantonio, E., Kaptoge, S., Wormser, D., Willeit, P., Butterworth, A. S., Bansal, S., Bonana-Kaylo, M., Boer, J., Brandslund, I., Brouwer, I. A., et al. (2015). Association of cardiometabolic multimorbidity with mortality. *The Journal of the American Medical Association* 314(1), 52–60. doi: 10.1001/jama.2015.7008.
- Didelez, V., and Sheehan, N. (2007). Mendelian randomization as an instrumental variable approach to causal inference. *Statistical Methods in Medical Research* 16(4), 309–330. doi: 10.1177/0962280206077743.
- Emdin, C. A., Khera, A. V., Natarajan, P., Klarin, D., Zekavat, S. M., Hsiao, A. J., and Kathiresan, S. (2017). Genetic association of waist-to-hip ratio with cardiometabolic traits, type 2 diabetes, and coronary heart disease. *The Journal of the American Medical Association* 317(6), 626–634. doi: 10.1001/jama.2016.21042.
- Gkatzionis, A., and Burgess, S. (2019). Contextualizing selection bias in Mendelian randomization: How bad is it likely to be? *International Journal of Epidemiology* 48(3), 691–701. doi: 10.1093/ije/dyy202.
- Hartwig, F. P., Davey Smith, G., and Bowden, J. (2017). Robust inference in summary data Mendelian randomization via the zero modal pleiotropy assumption. *International Journal of Epidemiology* 46(6), 1985–1998. doi: 10.1093/ije/dyx102.
- Hemani, G., Zheng, J., Elsworth, B., Wade, K. H., Haberland, V., Baird, D., Laurin, C., Burgess, S., Bowden, J., Langdon, R., et al. (2018). The MR-Base platform supports systematic causal inference across the human phenome. *eLife* 7, e34408. doi: 10.7554/eLife.34408.
- Hu, X., Zhao, J., Lin, Z., Wang, Y., Zhang, H., Lu, Q., and Yang, C. (2022). Mendelian randomization for causal inference accounting for pleiotropy and sample structure using genome-wide summary statistics. *Proceedings of the National Academy of Sciences* 119(28), e2106858119. doi: 10.1073/pnas.2106858119.

- Jiang, T., Gill, D., Butterworth, A. S., and Burgess, S. (2023). An empirical investigation into the impact of winner’s curse on estimates from Mendelian randomization. *International Journal of Epidemiology* 52(4), 1209–1219. doi: 10.1093/ije/dyac233.
- Jin, Y., Liang, J., Hong, C., Liang, R., and Luo, Y. (2023). Cardiometabolic multimorbidity, lifestyle behaviours, and cognitive function: a multicohort study. *The Lancet Healthy Longevity* 4(6), e265–e273. doi: 10.1016/S2666-7568(23)00054-5.
- Jones, D. S., and Podolsky, S. H. (2015). The history and fate of the gold standard. *The Lancet* 385(9977), 1502–1503. doi: 10.1016/S0140-6736(15)60742-5.
- Liu, Z., and Lin, X. (2018). Multiple phenotype association tests using summary statistics in genome-wide association studies. *Biometrics* 74(1), 165–175. doi: 10.1111/biom.12735.
- Locke, A. E., Kahali, B., Berndt, S. I., Justice, A. E., Pers, T. H., Day, F. R., Powell, C., Vedantam, S., Buchkovich, M. L., Yang, J., et al. (2015). Genetic studies of body mass index yield new insights for obesity biology. *Nature* 518(7538), 197–206. doi: 10.1038/nature14177.
- Loh, P.-R., Tucker, G., Bulik-Sullivan, B. K., Vilhjálmsson, B. J., Finucane, H. K., Salem, R. M., Chasman, D. I., Ridker, P. M., Neale, B. M., Berger, B., and Price, A. L. (2015). Efficient Bayesian mixed-model analysis increases association power in large cohorts. *Nature Genetics* 47(3), 284–290. doi: 10.1038/ng.3190.
- Ma, X., Wang, J., and Wu, C. (2023). Breaking the winner’s curse in Mendelian randomization: Rerandomized inverse variance weighted estimator. *The Annals of Statistics* 51(1), 211–232. doi: 10.1214/22-aos2252.
- Neeland, I. J., Turer, A. T., Ayers, C. R., Powell-Wiley, T. M., Vega, G. L., Farzaneh-Far, R., Grundy, S. M., Khera, A., McGuire, D. K., and de Lemos, J. A. (2012). Dysfunctional adiposity and the risk of prediabetes and type 2 diabetes in obese adults. *The Journal of the American Medical Association* 308(11), 1150–1159. doi: 10.1001/2012.jama.11132.
- Pierce, B. L., and Burgess, S. (2013). Efficient design for Mendelian randomization studies:

- Subsample and 2-sample instrumental variable estimators. *American Journal of Epidemiology* 178(7), 1177–1184. doi: 10.1093/aje/kwt084.
- Price, A. L., Patterson, N. J., Plenge, R. M., Weinblatt, M. E., Shadick, N. A., and Reich, D. (2006). Principal components analysis corrects for stratification in genome-wide association studies. *Nature Genetics* 38(8), 904–909. doi: 10.1038/ng1847.
- Purcell, S., Neale, B., Todd-Brown, K., Thomas, L., Ferreira, M. A. R., Bender, D., Maller, J., Sklar, P., de Bakker, P. I. W., Daly, M. J., and Sham, P. C. (2007). PLINK: A tool set for whole-genome association and population-based linkage analyses. *The American Journal of Human Genetics* 81(3), 559–575. doi: 10.1086/519795.
- Qi, G., and Chatterjee, N. (2019). Mendelian randomization analysis using mixture models for robust and efficient estimation of causal effects. *Nature Communications* 10(1), 1941. doi: 10.1038/s41467-019-09432-2.
- Robertson, D. S., Prevost, A. T., and Bowden, J. (2016). Accounting for selection and correlation in the analysis of two-stage genome-wide association studies. *Biostatistics* 17(4), 634–648. doi: 10.1093/biostatistics/kxw012.
- Rothman, K. J., and Greenland, S. (2005). Causation and causal inference in epidemiology. *American Journal of Public Health* 95(S1), S144–S150. doi: 10.2105/ajph.2004.059204.
- Sadreev, I. I., Elsworth, B. L., Mitchell, R. E., Paternoster, L., Sanderson, E., Davies, N. M., Millard, L. A., Smith, G. D., Haycock, P. C., Bowden, J., et al. (2021). Navigating sample overlap, winner’s curse and weak instrument bias in Mendelian randomization studies using the UK biobank. *medRxiv*. doi: 10.1101/2021.03.22.21253965.
- Sanderson, E., Richardson, T. G., Hemani, G., and Davey Smith, G. (2021). The use of negative control outcomes in Mendelian randomization to detect potential population stratification. *International Journal of Epidemiology* 50(4), 1350–1361. doi: 10.1093/ije/dyaa288.
- Sanderson, E., Glymour, M. M., Holmes, M. V., Kang, H., Morrison, J., Munafò, M. R., Palmer, T., Schooling, C. M., Wallace, C., Zhao, Q., and Davey Smith, G. (2022).

- Mendelian randomization. *Nature Reviews Methods Primers* 2, 6. doi: 10.1038/s43586-021-00092-5.
- Smith, G. D., and Ebrahim, S. (2003). ‘Mendelian randomization’: Can genetic epidemiology contribute to understanding environmental determinants of disease? *International Journal of Epidemiology* 32(1), 1–22. doi: 10.1093/ije/dyg070.
- Su, Y., Xu, S., Ma, Y., Yin, P., Hao, X., Zhou, J., Fung, W. K., Jiang, H., and Wang, P. (2024). A modified debiased inverse-variance weighted estimator in two-sample summary-data Mendelian randomization. *Statistics in Medicine* 43(29), 5484–5496. doi: 10.1002/sim.10245.
- Sullivan P F, Agrawal A, Bulik C M, et al. (2018). Psychiatric genomics: An update and an agenda. *The American Journal of Psychiatry* 175(1), 15–27. doi: 10.1176/appi.ajp.2017.17030283.
- Willer, C. J., Schmidt, E. M., Sengupta, S., Peloso, G. M., Gustafsson, S. et al. (2013). Discovery and refinement of loci associated with lipid levels. *Nature Genetics* 45(11), 1274–1283. doi: 10.1038/ng.2797.
- Xie, Z., Zhang, W., Wang, J., and Wu, C. (2025). Winner’s curse free robust Mendelian randomization with summary data. *Journal of the American Statistical Association*. Advance online publication. doi: 10.1080/01621459.2025.2587321.
- Xu, S., Wang, P., Fung, W. K., and Liu, Z. (2023). A novel penalized inverse-variance weighted estimator for Mendelian randomization with applications to COVID-19 outcomes. *Biometrics* 79(3), 2184–2195. doi: 10.1111/biom.13732.
- Ye, T., Shao, J., and Kang, H. (2021). Debiased inverse-variance weighted estimator in two-sample summary-data Mendelian randomization. *The Annals of Statistics* 49(4), 2079–2100. doi: 10.1214/20-aos2027.
- Zhang, L., Liu, L., Ji, J., Yan, R., Guo, P., Gong, W., Xue, F., Zhou, X., and Yuan, Z. (2025). Efficient Mendelian randomization analysis with self-adaptive determination

of sample structure and multiple pleiotropic effects. *The American Journal of Human Genetics*. 112(8), 1962–1978. doi: 10.1016/j.ajhg.2025.06.002.

Zhao, Q., Wang, J., Hemani, G., Bowden, J., and Small, D. S. (2020). Statistical inference in two-sample summary-data Mendelian randomization using robust adjusted profile score. *The Annals of Statistics* 48(3), 1742–1769. doi: 10.1214/19-AOS1866.

Zhao, Y., Zhuang, Z., Li, Y. et al. (2024). Elevated blood remnant cholesterol and triglycerides are causally related to the risks of cardiometabolic multimorbidity. *Nature Communications* 15(1), 2451. doi: 10.1038/s41467-024-46686-x.